Solar wind energy input during prolonged, intense northward interplanetary magnetic fields: A new coupling function

A. M. Du,[1] B. T. Tsurutani,[2] and W. Sun[3]

Received 2 April 2011; revised 23 September 2011; accepted 28 September 2011; published 14 December 2011.

[1] Sudden energy release (ER) events in the midnight sector auroral zone during intense (B > 10 nT), long-duration (T > 3 h), northward (N = B_z > 0 nT) IMF magnetic clouds (MCs) during solar cycle 23 (SC23) have been examined in detail. The MCs with northward-then-southward (NS) IMFs were analyzed separately from MCs with southward-then-northward (SN) configurations. It is found that there is a lack of ER/substorms during the N field intervals of NS clouds. In sharp contrast, ER events do occur during the N field portions of SN MCs. From the above two results it is reasonable to conclude that the latter ER events represent residual energy remaining from the preceding S portions of the SN MCs. We derive a new solar wind–magnetosphere coupling function during northward IMFs: $E_{NIMF} = \alpha N^{-1/12} V^{7/3} B^{1/2} + \beta V|Dst_{\min}|$. The first term on the right-hand side of the equation represents the energy input via "viscous interaction," and the second term indicates the residual energy stored in the magnetotail. It is empirically found that the magnetotail/magnetosphere/ionosphere can store energy for a maximum of ~4 h before it has dissipated away. This concept is defining one for ER/substorm energy storage. Our scenario indicates that the rate of solar wind energy injection into the magnetotail/magnetosphere/ionosphere for storage determines the potential form of energy release into the magnetosphere/ionosphere. This may be more important to understand solar wind–magnetosphere coupling than the dissipation mechanism itself (in understanding the form of the release). The concept of short-term energy storage is also applied for the solar case. It is argued that it may be necessary to identify the rate of energy input into solar magnetic loop systems to be able to predict the occurrence of solar flares.

Citation: Du, A. M., B. T. Tsurutani, and W. Sun (2011), Solar wind energy input during prolonged, intense northward interplanetary magnetic fields: A new coupling function, *J. Geophys. Res.*, *116*, A12215, doi:10.1029/2011JA016718.

1. Introduction

[2] It was well established that the mechanism of magnetic reconnection [*Dungey,* 1961; *Gonzalez and Mozer*, 1974] is the predominant means of solar wind energy transfer to the magnetotail/magnetosphere, especially for large energy release events such as magnetic storms [*Gonzalez and Tsurutani,* 1987; *Gonzalez et al.*, 1989, 1994; *Tsurutani et al.*, 1988; *Tsurutani and Gonzalez*, 1997; *Echer et al.*, 2008]. However, it is unclear if there is residual energy remaining in the magnetotail/magnetosphere system after a southward IMF interval, and if so, how much and for how long after injection? Is the vast magnetic energy in the magnetotail/magnetosphere a reservoir for energy release?

[3] *Zhou and Tsurutani* [2001], *Tsurutani and Zhou* [2003], and *Echer et al.* [2011] have examined specific cases of interplanetary shock triggering (or lack of triggering) of sudden magnetospheric midnight sector energy releases (ERs). They determined a critical duration of $\tau \sim 1$ 1/2 to 2 h of magnetotail/magnetosphere preloading. If there is substantial southward IMFs with $t < \tau$, then a sudden compression of the magnetosphere/magnetotail by a shock will lead to a sudden release of energy in the form of an ER. If there is not, then there will not be an ER. The arguments presented in the above works are that fresh solar wind energy must be put into the magnetosphere/magnetotail for ERs (and substorms) to occur, otherwise the energy will leak away within a short time τ. Thus, the enormous tail energy reservoir does not appear to be tapped in these cases. For high solar wind speed and high ion density conditions, the duration of the N part of south-north (SN) MCs [*Du et al.*, 2008; *Mannucci et al.*, 2008] would be ideal to test this idea further.

[4] In this paper, we use the term "ER" to indicate a sudden release of energy into the midnight sector auroral region. Many of the past papers on shock triggering of geomagnetic activity have called these ER events substorms [*Heppner*, 1955; *Schieldge and Siscoe*, 1970; *Kawasaki*

[1]Institute of Geology and Geophysics, Chinese Academy of Sciences, Beijing, China.
[2]Jet Propulsion Laboratory, California Institute of Technology, Pasadena, California, USA.
[3]Geophysical Institute, University of Alaska Fairbanks, Fairbanks, Alaska, USA.

0148-0227/11/2011JA016718

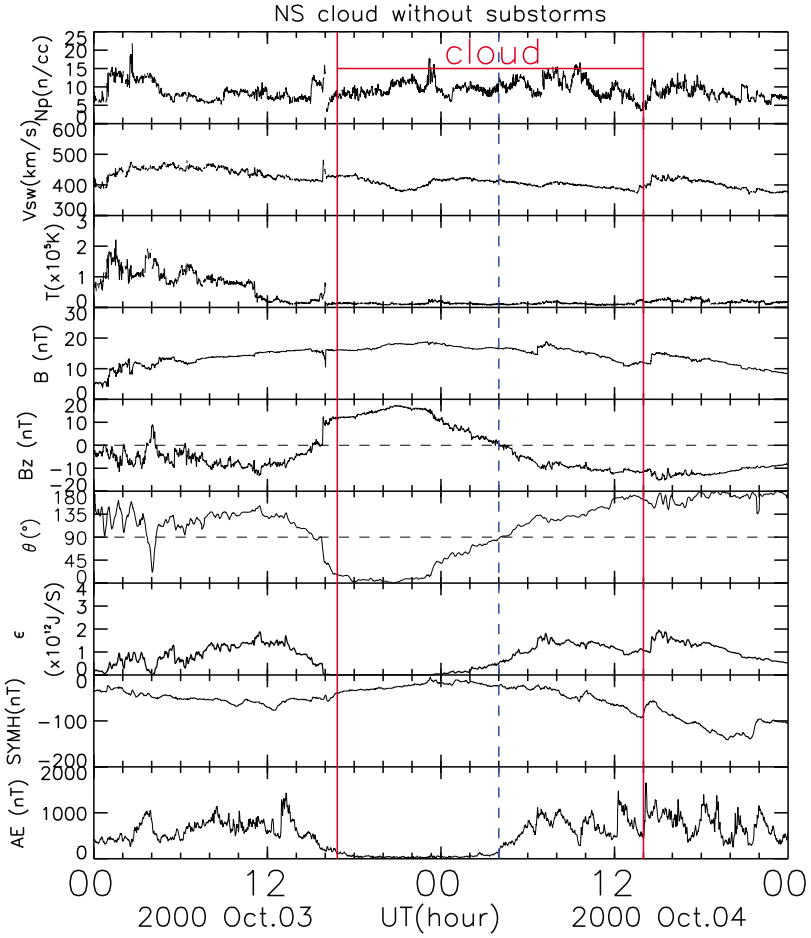

Figure 1. A typical example of the NS type of cloud on 2000 October 3–4. From top to bottom, the proton number density (N_p), velocity (V_{sw}), temperature (T) of the solar wind, the magnetic field magnitude (B), the GSM Bz component, the clock angle (θ) of the IMF (described below), the ε function, the geomagnetic $SYMH$ index and the AE index during October 3–4, 2000.

et al., 1971; *Burch*, 1972; *Tsurutani et al.*, 1999; *Zhou and Tsurutani,* 2001; *Tsurutani et al.*, 2001; *Tsurutani and Zhou*, 2003; *Echer et al.*, 2011]. Because there is some controversy about whether this energy release (ER) is indeed a "classic" substorm or some other related phenomenon [*Henderson et al.*, 1996; *Chua et al.*, 2001; *Lyons*, 2000; *Meurant et al.*, 2005], we use the neutral term ER throughout this paper. The main point of this paper is that sometimes there is midnight sector energy release and sometime there is not. This is the main focus of the paper, not the form that the energy release takes. We do describe the auroral forms in these sudden bursts of energy release so that the reader can decide for himself/herself whether they are "classic" substorms or not.

[5] *Tsurutani and Gonzalez* [1995] have examined solar wind energy input into the magnetosphere during intervals of intense and long duration northward IMFs. From their empirical studies, they found that the fractional amount of solar wind (ram) energy input into the magnetosphere during northward IMFs is sometimes quite low, units of ~1 to ~4 × 10^{-3}. They surmised that the input mechanism could either be a low level of magnetic reconnection or some form of viscous interaction.

[6] It is the purpose of this present work to extend the above ideas further. We will examine the MC events that occurred from 1996 through 2007 in solar cycle 23 (SC23). However, unlike the *Tsurutani and Gonzalez* [1995] effort, we will go further and distinguish NS events from SN event. Each group will be studied separately. It will be demonstrated that the geomagnetic activity in the magnetosphere during the northward IMF intervals is different for these two different cases. Second, a scenario of energy storage will be presented. A new solar wind–magnetosphere coupling relationship will be presented for magnetic reconnection during northward IMFs.

2. Observations of ER Events During Northward IMF Intervals in Magnetic Clouds

2.1. ER Occurrence During N Intervals in NS MCs?

[7] Figure 1 shows, from top to bottom, the proton number density (N_p), velocity (V_{sw}), temperature (T) of the solar wind, the magnetic field magnitude (B), the GSM Bz component, the clock angle (θ) of the IMF (described below), the ε-function [*Perreault and Akasofu*, 1978], the geomagnetic

SYMH index and the *AE* index during October 3–4, 2000. The clock angle θ is defined by IMF B_y and B_z as:

$$\theta = \tan^{-1}\left(|B_y/B_z|\right) \text{ if } B_z \geq 0; \quad \theta = \pi + \tan^{-1}\left(|B_y/B_z|\right) \text{ if } B_z < 0 \tag{1}$$

The ε-function is a solar wind–magnetosphere coupling function [*Perreault and Akasofu*, 1978] and can be written as

$$\varepsilon = V_{SW}B^2 \sin^4(\theta/2) l_0^2 \times 10^{-7}\left(\mathrm{Js}^{-1}\right) \tag{2}$$

where the constant l_0 is taken as 7 R_E, where a R_E is an Earth radius.

[8] A magnetic cloud (MC) is defined as a region in the solar wind with enhanced magnitude of magnetic field, smooth rotation of the magnetic field vector with a lack of discontinuities and waves and with a low plasma temperature [*Burlaga et al.*, 1981; *Tsurutani et al.*, 1988; *Tsurutani and Gonzalez*, 1994]. In this paper, the identification of magnetic cloud events and its boundaries was adopted from *Lepping et al.* [2006]. Two red vertical lines indicate the beginning and end of a MC occurring from 1600 UT, October 3 to 1400 UT, October 4, 2000. A blue dash line indicates the time at which the IMF *Bz* component changed from northward (positive values) to southward (negative values). This occurred at ~0400 UT. The data were shifted forward by 42 min (calculated using the measured solar wind speed and the distance between ACE and the Earth). Thus the solar wind convection delay from ACE to the Earth was removed.

[9] It can be noted that the geomagnetic activity is exceptionally quiet (*AE* < 200 nT, *Dst* > −20 nT) during the N part of the MC from 1600 UT of October 3 to 0400 UT of October 4. In contrast, the geomagnetic activity became enhanced and multiple *AE* events with *AE* > 1000 nT took place after the IMF turned southward at ~0400 UT of October 4. The ε-function was very low (<1 × 10^{11} Js^{-1}) during the N part of the MC, whereas it increased to ~2 × 10^{12} Js^{-1} during the following S part of the MC.

2.2. ER Occurrence During N Intervals in SN MCs

[10] Figure 2 contains much of the same interplanetary parameters and geomagnetic indices as in Figure 1, but for a MC SN event. The interval shown is from 0000 UT, August 12 to 2400 UT, August 13, 2000. The figure contains the solar wind N_p, V_{sw}, *T*, *B*, B_z, θ values and the *SYMH,* and *AE* indices. Several new parameters have been added: $d\Phi_{MP}/dt$ (defined below), E_{VIS}, and the tilt angles of the magnetic field in the plasma sheet. Solar wind plasma and IMF parameters were observed by the ACE satellite [*Stone et al.*, 1998], and the data were shifted forward by 36 min to take into account the solar wind convection delay to the Earth.

[11] $d\Phi_{MP}/dt$ is the magnetopause magnetic flux cutting rate. An expression for this has been given by *Newell et al.* [2007, 2008] as:

$$d\Phi_{MP}/dt = V_{SW}^{4/3} B^{2/3} \sin^{8/3}(\theta/2) \tag{3}$$

The ε-function and $d\Phi_{MP}/dt$ give quantitative values for the solar wind–magnetosphere energy coupling by magnetic reconnection at the dayside magnetopause.

[12] E_{VIS} and AE_{VIS}, were calculated using the TG method [*Tsurutani and Gonzalez*, 1995]. This represents the energy input into the magnetosphere via "viscous interaction" and the *AE* index contributed by the "viscous interaction" process, respectively. These two terms are defined in section 3.2.

[13] In Figure 2, it is noted that after the IMF turned northward at 1732 UT, ε was ~10^{12} Js^{-1} and E_{vis} was ~0.5 × 10^{11} Js^{-1}. In Figure 2 (bottom), the AE_{vis} index is much lower than the *AE* index.

[14] The tilt angle of the magnetic field in the plasma sheet was observed by GOES 8. The tilt angle is calculated using the following expression:

$$\vartheta_{tilt} = \tan^{-1}\left[B_z/\sqrt{\left(B_x^2 + B_y^2\right)}\right], \tag{4}$$

A SN MC structure is identified in Figure 2 between 0520 UT, August 12 and 2200 UT, August 13, 2000. The beginning and end are indicated by two vertical red lines. This identification follows previous works by *Xue et al.* [2005], *Nieves-Chinchilla et al.* [2005], *Lepping et al.* [2006], and *Wang et al.* [2006]. A major magnetic storm developed when the S portion of a MC impinged onto the magnetosphere. In this case the main phase of the storm started to develop at ~0210 UT on August 12, 2000 and reached the minimum negative *SYMH* value of −240 nT at ~1000 UT. During the recovery phase of the storm, the IMF B_z turned northward at 1732 UT on August 12, 2000 (indicated by the vertical blue dash line) and remained northward for over 12 h.

[15] During the storm recovery phase, the *AE* index had abrupt increases at ~0005 UT and ~0325 UT on August 13, 2000. These two events had maximum *AE* values of 647 nT and 561 nT, respectively. There was a change in the dipole tilt for the first event but a lack of a change in the second event (the GOES 8 spacecraft was located on the dusk side for the second event, a location that may have missed the magnetotail depolarization). These two events are interpreted as the occurrence of two ERs.

[16] There are more *AE* events just after the "northward turning" of IMF. *Lee et al.* [2010] identified an ER onset at 1910 UT for about 1.6 h after the "northward turning" of the IMF. We did not classify this ER as part of the geomagnetic activity event during prolonged IMF conditions. During this period, the former ERs did not recover to quiet level (<500 nT). The IMF *Bz* was not sufficiently strong, but turned southward around the onset of the ER.

[17] The IMAGE Wideband Imaging Camera (WIC) UV images for the first event at ~0005 UT of 13 August 2000 are shown in Figure 3. In each north pole image, noon is at the top and dawn is to the right. The magnetic pole is at the center and the concentric rings demark 10° in MLAT. The imaging shown has a cadence of 2 min 3 s. The images start at the top left and proceed to the right.

[18] The first image of Figure 3 shows the pre-onset auroral oval. There is some faint (shown in blue) aurora from 18 to 22 MLT and from 60° to 70° MLAT. The ER onset time is identified at ~0002:59 UT by the intensification in the local time-MLAT region mentioned above [*Frey et al.*, 2004]. By 0013:12 UT the aurora had extended from ~2100 to 0200 MLT and 60° to 70° MLAT (primarily an eastward expansion). After that time, the aurora faded. There

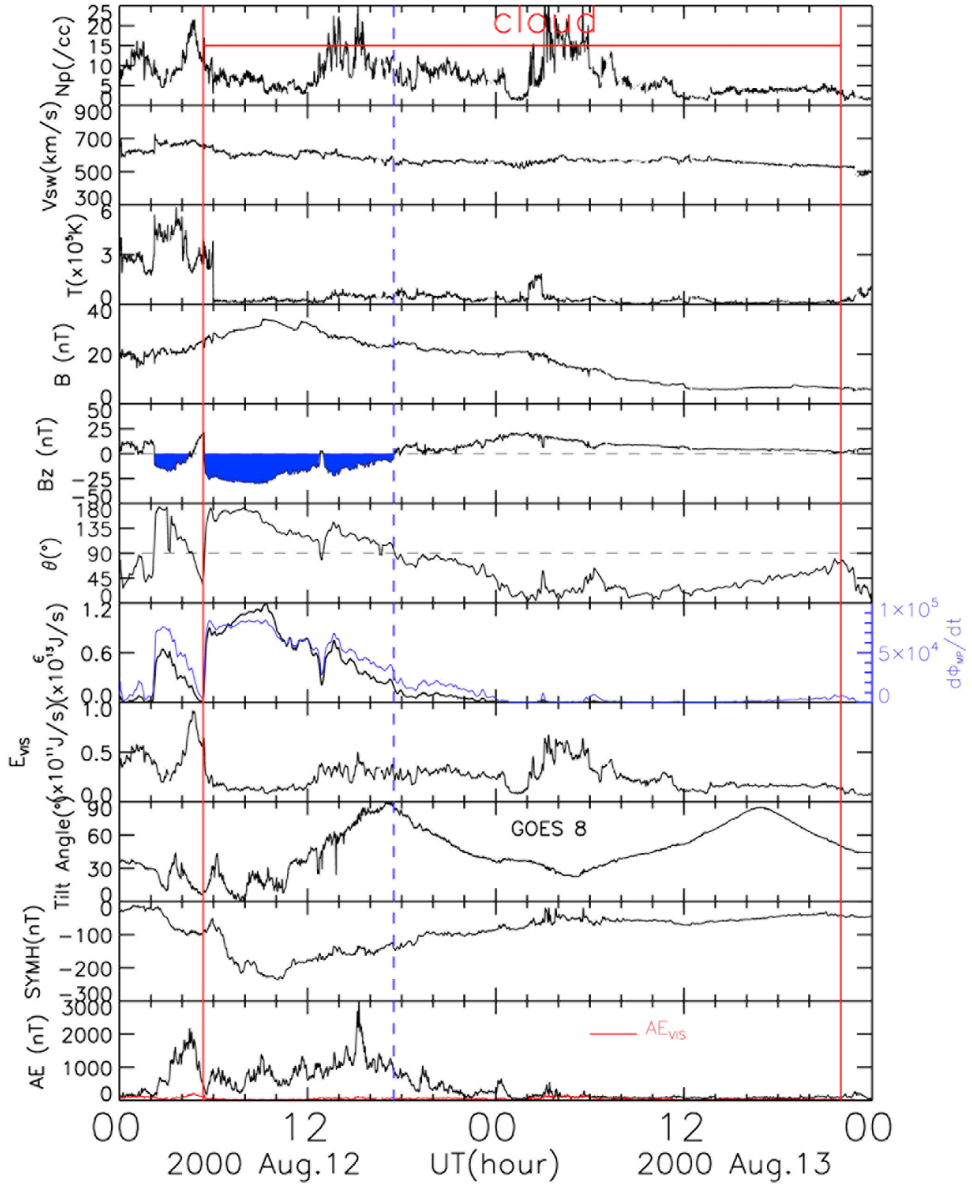

Figure 2. The proton number density (*Np*), solar wind velocity (*Vsw*), temperature (*T*), *B*, *Bz*, clock angle (θ) of IMF, ε, $d\Phi_{MP}/dt$, E_{VIS}, tilt angles of magnetic field in the plasma sheet, the SYMH index and the AE index from 0000 UT, August 12 to 2400 UT, August 13, 2000. Two red vertical lines indicate the boundaries of the magnetic cloud, and the blue vertical dash line indicates the southward turning of IMF.

are unfortunately no available confirming auroral observations for the second ER at 0325 UT.

[19] Figure 4 shows one more example of a SN MC from 1200 UT, July 15 to 1200 UT, July 16, 2000. A SN MC impinged upon the Earth between ~1900 UT, July 15 and ~0900 UT, July 16, 2000. Solar wind plasma and IMF parameters were observed by the ACE satellite, and the data were shifted forward by 23 min to take into account the solar wind convection delay. The MC is again identified by the vertical red lines. The S portion of the SN MC caused a major magnetic storm with a minimum *SYMH* value of −350 nT at 2200 UT on July 15, 2000. The IMF B_z turned to northward at ~0050 UT on July 16, 2000 (indicated by the vertical blue dash line) and remained northward for more than 12 h afterwards.

[20] After the onset of the N interval, the ε function was ~10^{12} Js^{-1} and E_{vis} was ~10^{11} Js^{-1}. In Figure 4 (bottom), it is noted that the AE_{vis} index is much lower than the *AE* index. Three *AE* enhancement events occurred at ~0101 UT, ~0345 UT, and ~0420 UT of 16 July 2000 with peak *AE* values of ~1100 nT, ~673 nT, and ~1000 nT, respectively. These three events occurred during the N portion of the MC.

[21] Magnetic field depolarization can be seen by the magnetic field data of GOES 8, which was located in the midnight sector. The dipole tilt angle in Figure 4 sharply increased at ~0101 UT, and again at ~0420 UT.

[22] The IMAGE/FUV auroral images for this event are shown in Figure 5. The format is the same as in Figure 3. The first row of the Figure 5 images shows the ongoing auroral expansion process for the first ER. The onset time of

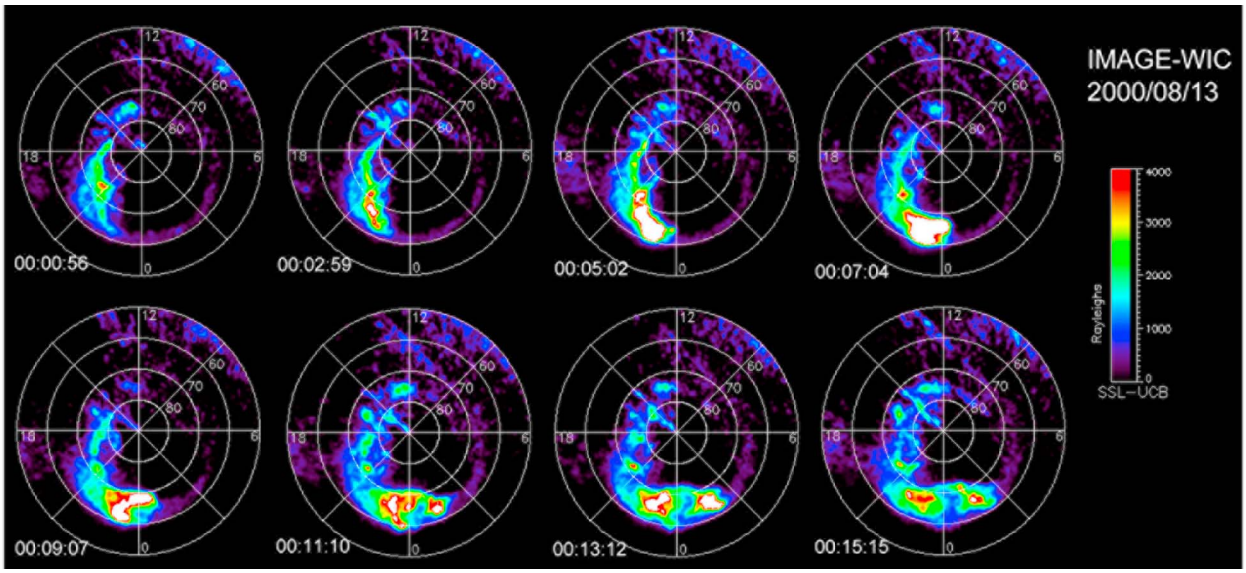

Figure 3. The Wideband Imaging Camera (WIC) images from IMAGE satellite during ER on August 13, 2000.

~0101 UT is not shown but the interval from 0101:43 UT to 0111:56 UT indicates the ER intensity in the premidnight sector (unfortunately the IMAGE viewing misses part of the auroral activity). In the second row of images, the aurora brightening was observed at ~0343:09 UT, and the auroral expansion at ~0345:12 UT, corresponding to the second ER onset time. In the third row of images, the ER onset occurred in the first image at ~0415:51 UT with auroral intensification at ~1800 MLT located at 70° MLAT. The third onset time is identified by the *AE* index and the dipole tilt angle. By the last image of the third row at 0428:07 UT, the aurora has extended to cover the spatial location MLT = 1900 to 0000 MLT and MLAT = 60° to ~78°. The ER morphology of the latter event was similar to a typical substorm under more normal southward IMF conditions.

3. Energy Coupling Between the Solar Wind and Magnetosphere

3.1. The N Portions of NS MCs

[23] A total of 14 NS MC events were identified throughout SC23 (1996–2008) with a criteria with $B_n > 10$ nT and T > 3 h. Parameters for NS cloud events such as date, average value of U_T, U_I, B, V_{sw}, N and θ are listed in Table 1. The averaged values were obtained using the 1 min resolution data during the N part of NS MCs.

[24] U_T is the total energy dissipation and can be written as [*Akasofu*, 1981]

$$U_T = U_R + U_I \tag{5}$$

where U_R and U_I are the energy deposition rates in the ring current and in the polar ionosphere, respectively. U_R is defined as:

$$U_R = -4 \times 10^7 \left(\frac{\partial D^*_{st}}{\partial t} + \frac{\partial D^*_{st}}{\tau_r} \right) (\text{J s}^{-1}) \tag{6}$$

where Dst^* (nT) is the solar wind pressure corrected ring current index [*Gonzalez et al.*, 1989]. In the above expression, $Dst^* = Dst - b\sqrt{p} - c$, where b = 10.5 nT(nPa)$^{-1/2}$ and c = 22 nT. The time constant τ_r is the life time of the ring current particles. Following *Akasofu* [1981], τ_r takes two different values for strong storm and non-storm/weak storm conditions:

$$\tau_r = \begin{cases} 20\text{h} & \text{for } \varepsilon < 5 \times 10^{11} \text{ J s}^{-1} \\ 1\text{h} & \text{for } \varepsilon > 5 \times 10^{11} \text{ J s}^{-1} \end{cases} \tag{7}$$

The ionospheric energy deposition rate, U_I, can be approximated [*Akasofu,* 1981] by

$$U_I = U_A + U_J = 3 \times 10^{15} AE \text{ (nT) J s}^{-1} \tag{8}$$

where U_A is the auroral energy deposition, and U_J the rate of Joule heating. In the above, the *AE* index is standardly used as a proxy for both the magnitudes of U_A and U_J.

[25] Figure 6 shows the correlation of U_T with the interplanetary parameters B, V_{SW}, N and θ for the N portion of the NS MCs. It is interesting to note that U_T has a good linear correlation with the solar speed V_{sw}. This is shown in Figure 6b. The correlation coefficient is 0.98, and the slope is 3.62×10^{-9}.

[26] *Vasyliunas et al.* [1982] suggested a solar wind–magnetosphere energy transfer formula for the viscous coupling.

$$P_{Vasyliunas} = N^{1/2-b/3} V_{SW}{}^{5/2+b/3} F(M_A^2, \theta) M_E^{1/2-b/3} \mu_0^{1/6-b/3} (m/e)^{1/2+b} \tag{9}$$

where N is proton density, V_{sw} is solar wind velocity, B is magnitude of IMF, $F(M_A^2, \theta) = M_A^{-1/2} G(\theta)$ is an unspecified dimensionless function of the dimensionless ratios, M_A ($=\sqrt{\mu_0 N V_{SW}{}^2 / B^2}$) is the Alfvén-Mach number, M_E (~7.95×10^{15} T·m^3) the Earth's magnetic dipole moment, μ_0 is vacuum permeability, m and e are the proton charge and mass, respectively.

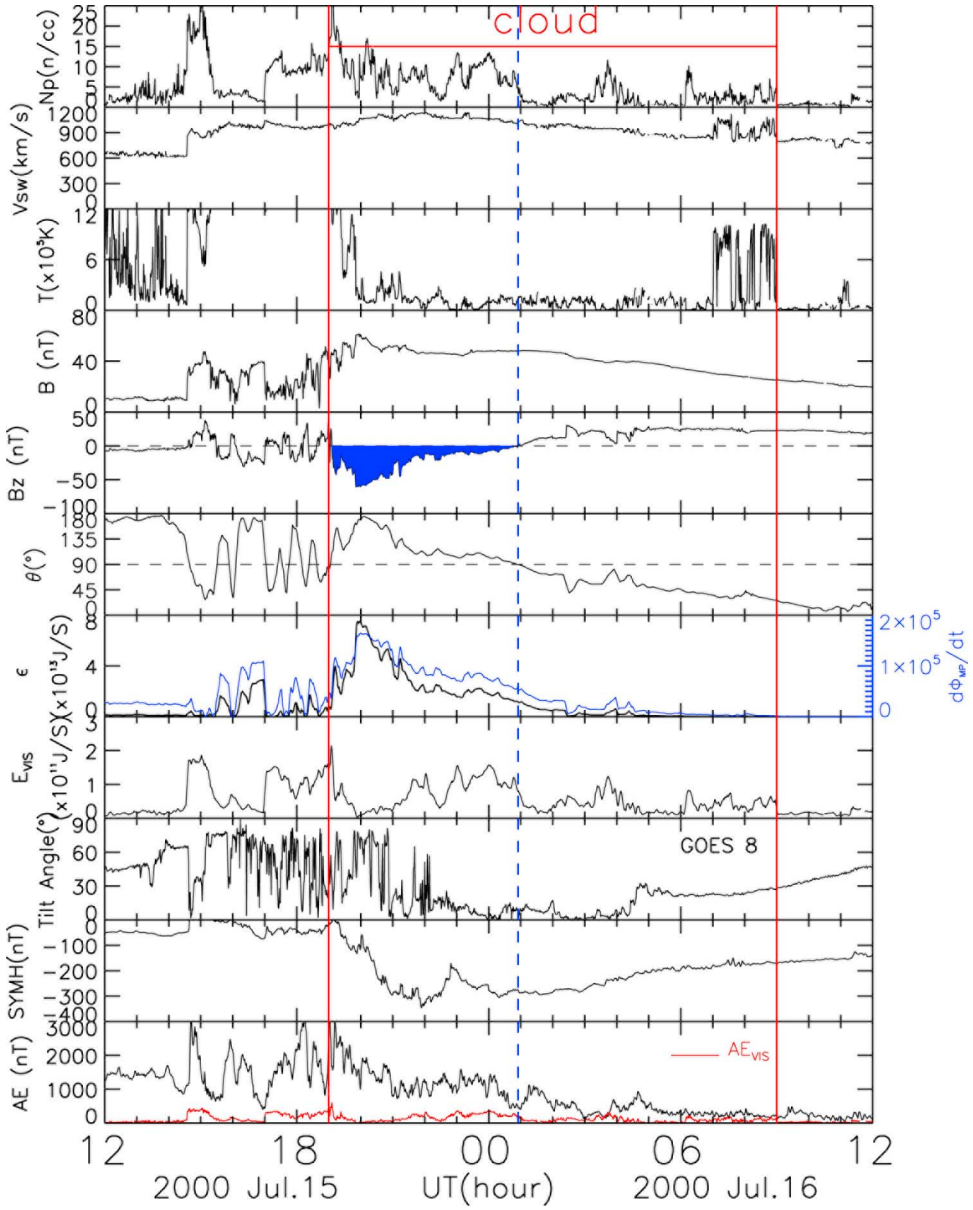

Figure 4. The proton number density (*Np*), solar wind velocity (*Vsw*), temperature (*T*), *B*, *Bz*, clock angle (θ) of IMF, ε, $d\Phi_{MP}/dt$, E_{VIS}, tilt angles of magnetic field in the plasma sheet, the SYMH index and the AE index from 1200 UT, July 15 to 1200 UT, July 16, 2000. Two red vertical lines indicate the boundaries of the magnetic cloud.

[27] Here, we set $G(\theta) = 1$. Figure 7 shows the correlation of U_T with $P_{Vasyliunas}$ for b = 0, 0.5 and 1.0, respectively. The highest correlation coefficient is 0.86 for a value b = 1.

[28] Setting b = 1, equation (9) can be written as:

$$P_{Vasyliunas} = \alpha N^{-1/12} V_{SW}^{7/3} B^{1/2} \tag{10}$$

where the coefficient, $\alpha = 9.42$, is a constant estimated by an experimental fit between $P_{Vasyliunas}$ and U_T. For the 2001 April 4 event, V_{SW} is >750 km/s, and the $P_{Vasyliunas}$ and U_T values are much larger than that for other events. Thus, the correlation coefficients and slope of the linear fit in Figure 6 could be mainly controlled by the two points of the 2001 April 4 and 2004 September 9 events. Indeed, the correlation coefficients and slope of U_T with $P_{Vasyliunas}$ (with the exclusion of the 2001 April 4 event and 2004 September 9 events) are 0.42 and 31.4, respectively.

3.2. The N Portion of SN MCs

[29] In Figure 2, the S portion of SN MC beginning at the first red line and ending at the dash blue line, through magnetic reconnection, causes the main phase of the magnetic storm. During the main phase, many ERs took place, indicated by the *AE* index variations. During the 8 h following the end of the southward IMF (the dashed blue line), the IMF *Bz* remained northward. Some ERs occurred during this latter interval of the storm recovery phase. This is the topic of focus in this section.

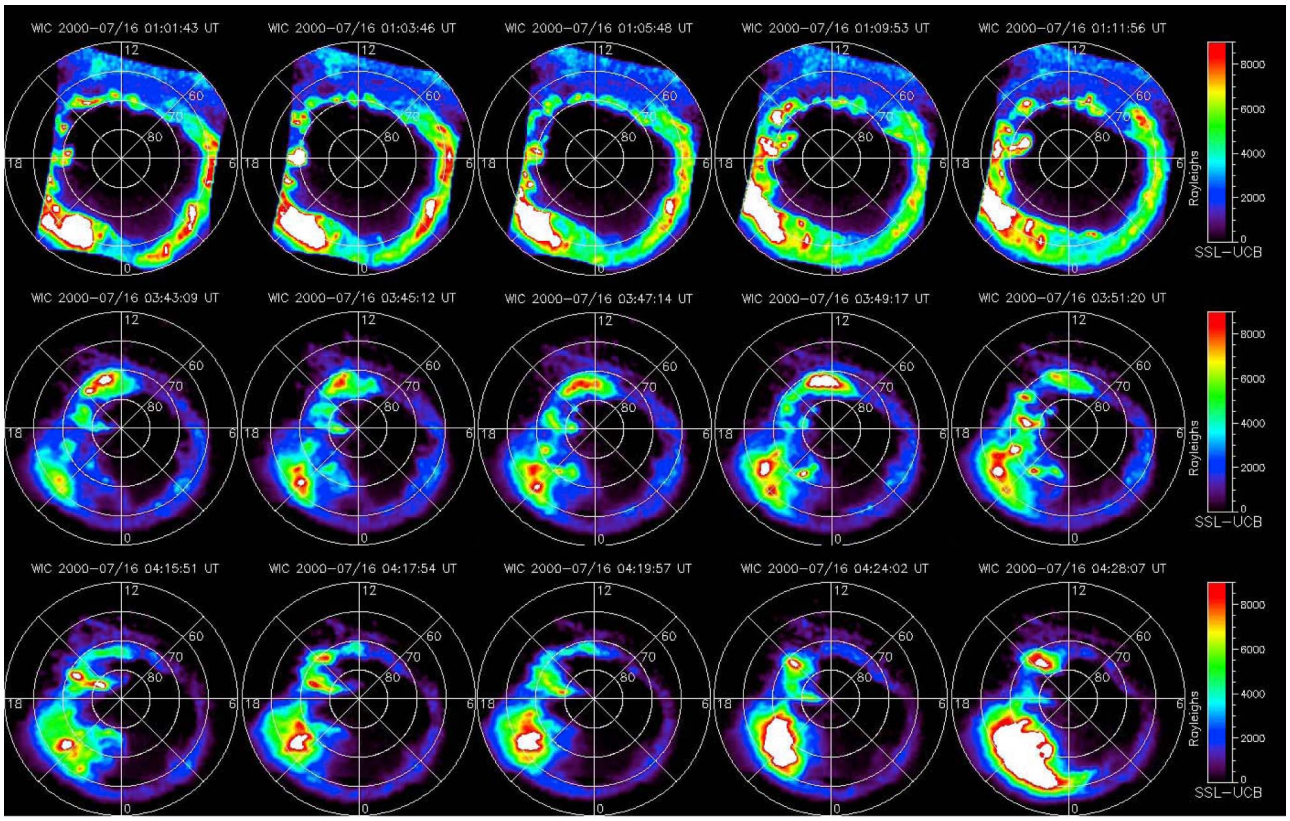

Figure 5. The Wideband Imaging Camera (WIC) images from IMAGE satellite during ER on July 16, 2000.

[30] *Tsurutani and Gonzalez* [1995] found that the typical efficiency of solar wind energy input into the Earth's magnetosphere via "viscous interaction" [*Axford and Hines*, 1961] is 1.0 to 4.0 × 10^{-3}, 100 to 300 times less efficient than that during periods of intense southward IMFs. The AE_{vis}, as a part of the *AE* index, which is attributed to "viscous interaction" can be estimated as following.

[31] First, the cross-sectional area of the magnetosphere can be calculated by using the formula

$$Area = \pi(1.1 \times R_{SO})^2 \tag{11}$$

where the nose of the magnetopause distance to the center of the Earth is in Earth-radii, R_{SO}. An expression for this distance given in terms of the solar wind pressure *P* and the IMF *Bz* has been derived by *Shue et al.* [1997].

[32] The incident solar wind energy flux in erg cm^{-2} s^{-1} is estimated by using formula $\frac{1}{2}MNV_{SW}^3$, where MN is the total proton plus helium mass density. The total energy flux impinging on the dayside magnetosphere, E_T, is calculated by

$$E_T = Area \times \frac{1}{2}MNV_{SW}^3 \tag{12}$$

Table 1. NS Cloud Events

Number	Date[a]	Average U_T (10^{10} J/s)	Average U_I (10^{10} J/s)	Average B (nT)	Average V_{SW} (km/s)	Average N (n/cc)	Average θ (deg)	Minimum Dst (nT)	Maximum AE (nT)
1	2000/10/03	2.37	1.83	17.1	409.2	9.2	11.8	−62	180
2	2001/04/04	11.29	6.48	14.3	731.3	4.2	5.1	−20	331
3	2002/03/19	1.94	1.21	14.3	366.1	1.1	4.1	−17	44
4	2002/08/02	2.55	2.55	12.7	507.0	5.2	6.0	−71	146
5	2002/10/01	2.06	1.73	22.5	364.2	7.5	11.5	−35	41
6	2003/06/17	4.03	4.03	8.4	471.5	6.1	7.0	−38	129
7	2004/04/04	2.23	1.27	16.5	415.0	7.8	13.8	−49	65
8	2004/08/29	3.14	1.17	9.4	408.0	7.0	7.9	−4	44
9	2004/11/09	13.79	13.44	38.0	805.6	7.7	9.8	−223	723
10	2006/02/05	1.29	0.60	7.9	352.0	15.3	20.7	6	27
11	2006/04/13	2.92	1.74	15.8	523.0	4.6	9.2	−6	104
12	2006/09/30	1.79	1.30	17.5	396.6	13.5	15.3	−7	53
13	2007/05/22	5.42	0.92	9.9	441.6	4.6	5.9	9	58
14	2007/11/20	3.47	1.44	14.6	452.7	8.4	14.6	−1	126

[a]Date format: yyyy/mm/dd.

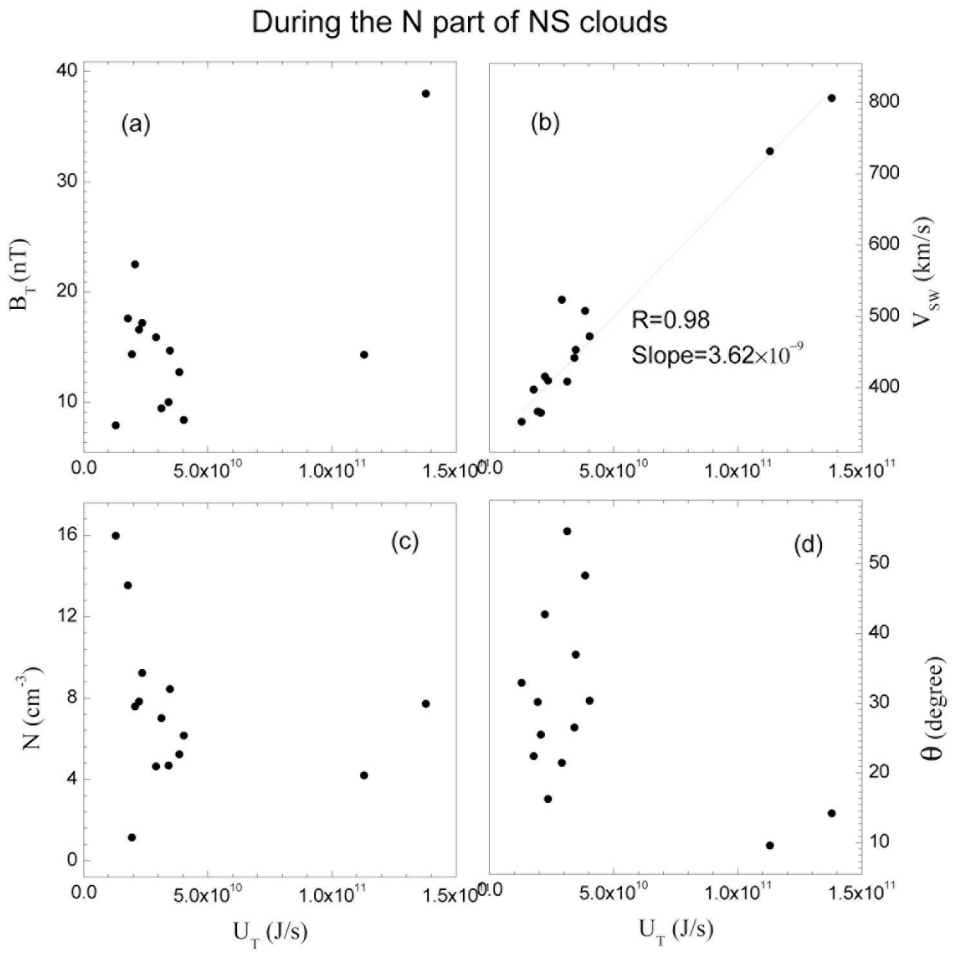

Figure 6. The correlation of the total energy dissipation (U_T) with the interplanetary parameters of B, V_{SW}, N and θ for the N portion of the NS MCs.

A lower efficiency limit (2.0×10^{-3}) [*Tsurutani and Gonzalez*, 1995] is applied to estimate the energy dissipation within the magnetopause [*Akasofu*, 1981].

$$E_{VIS} \approx 1.5 \times 10^{-3} \times E_T = U_T = U_R + U_A + U_J \qquad (13)$$

The U_I should be a part of energy dissipation of ERs in the ionosphere, $U_I = 2/3U_T$ [*Akasofu,* 1981]. Finally, the AE_{VIS} can be obtained by:

$$AE_{VIS} = \frac{2}{9} \times 10^{-15} U_T \text{ (nT)} \qquad (14)$$

After the IMF turned northward for the event in Figure 2, there was little electromagnetic energy input from the solar wind, as shown by $\varepsilon \sim 10^{12}$ J/s and a small amount of kinetic energy by viscous interaction as shown by $E_{VIS} \sim 10^{11}$ J/s and by the AE_{VIS} index with a red line in Figures 2 and 4 (bottom). The total input energy is not enough for the energy dissipation through an ER.

[33] For the SN MCs, it is implied that a great amount of energy has been stored in the magnetosphere during the leading part with southward IMF *Bz* accompanied by a storm [*Du et al.*, 2008; *Mannucci et al.*, 2008]. Then the stored energy is released during the N part of the SN cloud providing energy for occurrence of ERs. The energy dissipation within the magnetosphere also includes new energy input contributed by "viscous interaction" [*Tsurutani and Gonzalez*, 1995] or IMF *By* reconnection [*Lee et al.*, 2010] during the N part of the SN clouds.

[34] Figures 8a–8d show the correlation of the *AE* index to the magnitude of the IMF (B), clock angle (θ), solar wind speed (V_{SW}), and the *Dst* index, respectively. The black solid circles represent the events with $V_{SW} > 700$ km/s. The red solid circles represent events with $V_{SW} < 700$ km/s. The results demonstrate that no single parameter is well-correlated with the maximum *AE* value during ERs within northward IMF. However, it should be noted that V_{SW} (>700 km/s) and *Dst* have better correlations with the *AE* index than other parameters.

[35] The viscous coupling function, $P_{Vasyliunas}$, can be used as a baseline for the energy input. In order to estimate the energy stored in the magnetotail, $P_{Vasyliunas}$ is deduced from the total energy dissipation, U_T, during the N part of the SN clouds. Figure 9a shows the relationship between U_T and $P_{Vasyliunas}$ for SN cases. Eight ER events of Table 2 were analyzed. For the 2003 October 31 event, the data of the solar wind ion density are not available, thus we cannot estimate the pure energy stored (from our model) in the

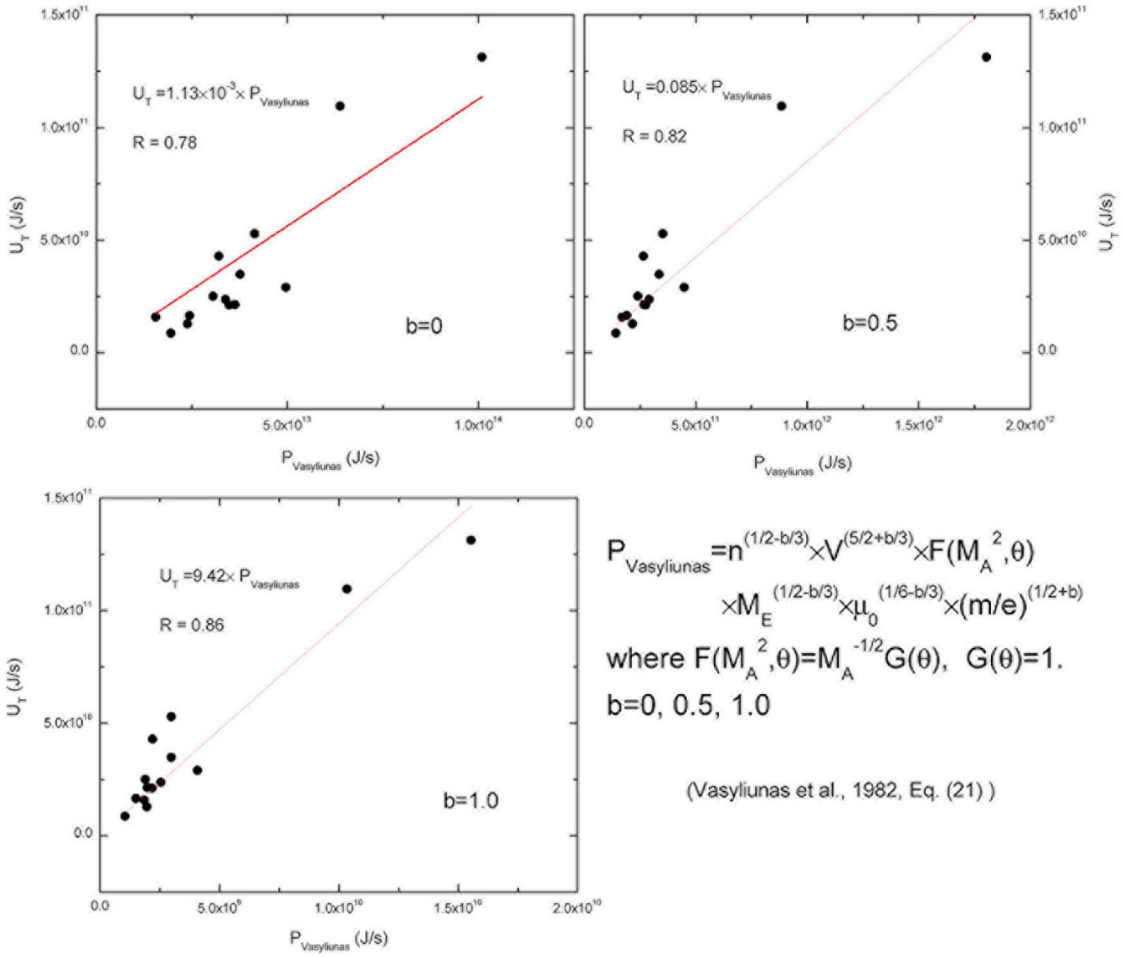

Figure 7. The correlation of U_T with $P_{Vasyliunas}$ for b = 0, 0.5 and 1.0 cases, respectively.

magnetotail. For the two ER events on 2000 August 12–13 and three ER events 2000 July 15–16 listed in Table 2, the two ERs with maximum *AE* were shown in Figure 9, respectively. It is noted that the $P_{Vasyliunas}$ is about 1.0 × 10^{-3} less than U_T. The stored energy in magnetosphere U_T - $P_{Vasyliunas}$ is well correlated with $V|Dst|_{\min}$ for ERs during the N part of the SN MC as shown in Figure 9b.

[36] We thus proposed a new solar wind–magnetosphere energy coupling function, E_{NIMF}. The expression is:

$$Enimf = \alpha N^{-1/12} V^{7/3} B^{1/2} + \beta V Dst_{\min} \qquad (15)$$

Where α = 9.42, and β = 1.64. The first term of the right side represents the energy coupling via "viscous interaction," and the second term indicates the energy stored in the magnetotail after a southward IMF interval.

3.3. The N Portion of NS and SN MCs Without ERs

[37] The minimum *Dst* and maximum *AE* index during the prolonged N part of NS MCs were listed in Table 1. There was a major geomagnetic storm (*Dst* ~ −223 nT) on November 9, 2004. The N part of NS MC was involved in the recovery phase of this storm, and the high *AE* (~723 nT) was also in the recovery phase of a storm during 1910~2130 UT on November 9, 2004. Except this event on November 9, 2004, the geomagnetic activity was very weak (*Dst* > −80 nT and *AE* < 400 nT) during the N part of NS MCs. It is noted that the solar wind speed was not very high.

[38] Table 3 gives 19 SN cloud events without ERs during the prolonged northward parts occurring in SC23. For these events, the magnitude of IMF was from 8.4 nT to 23.1 nT, the maximum solar wind speed was between 317 km/s and 625 km/s, *Dst* from 0 to −139 nT, and all *AE* values were less than 400 nT. For the event on April 29, 2001, the solar wind speed was about 625 km/s, the minimum *Dst* was −41 nT, while the *AE* index was only 118 nT. For these SN cloud events, the *V*•*Dst* is very small, the energy input by "viscous interaction" and the energy stored in the magnetotail after a southward IMF interval is very small and insufficient for an ER event.

4. Discussion

[39] The characteristics of ERs during prolonged northward IMF intervals (N intervals) are summarized below.

[40] 1. All ERs identified in this study took place in the N part of SN MCs and during the recovery phases of geomagnetic storms.

[41] 2. The ERs above were typically moderate in intensity with *AE* ~ 500 to 1500 nT. In the case that there is a series of ERs, the peak intensities typically decayed with time.

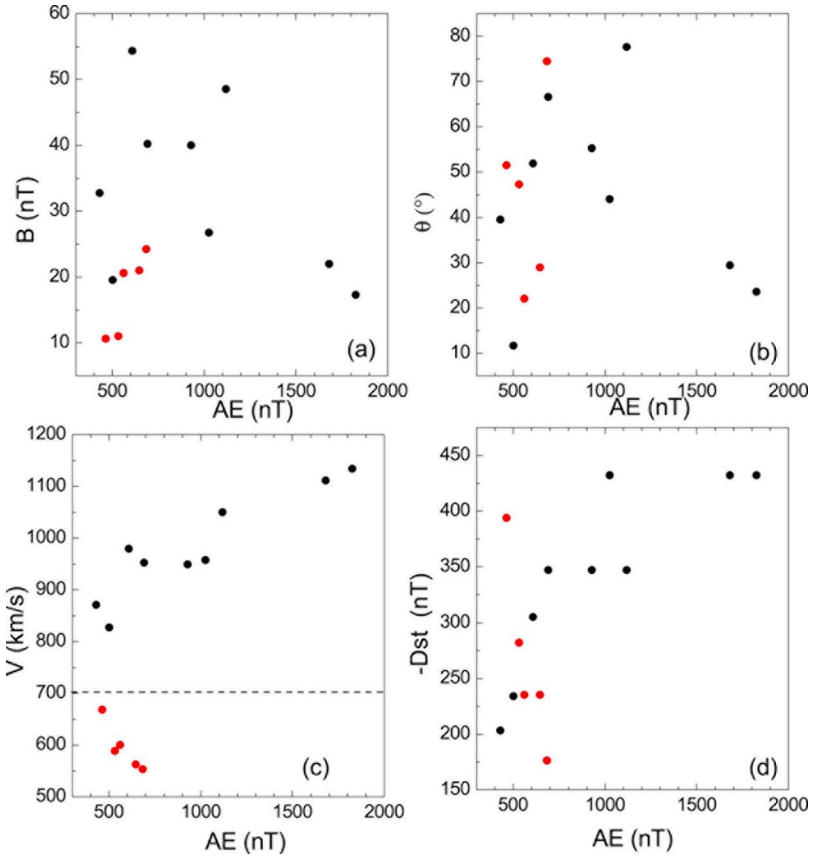

Figure 8. The correlation of the *AE* index to magnitude of IMF (*B*), clock angle (θ), solar wind speed (*V*), and the *Dst* index during the N part of SN cloud, respectively.

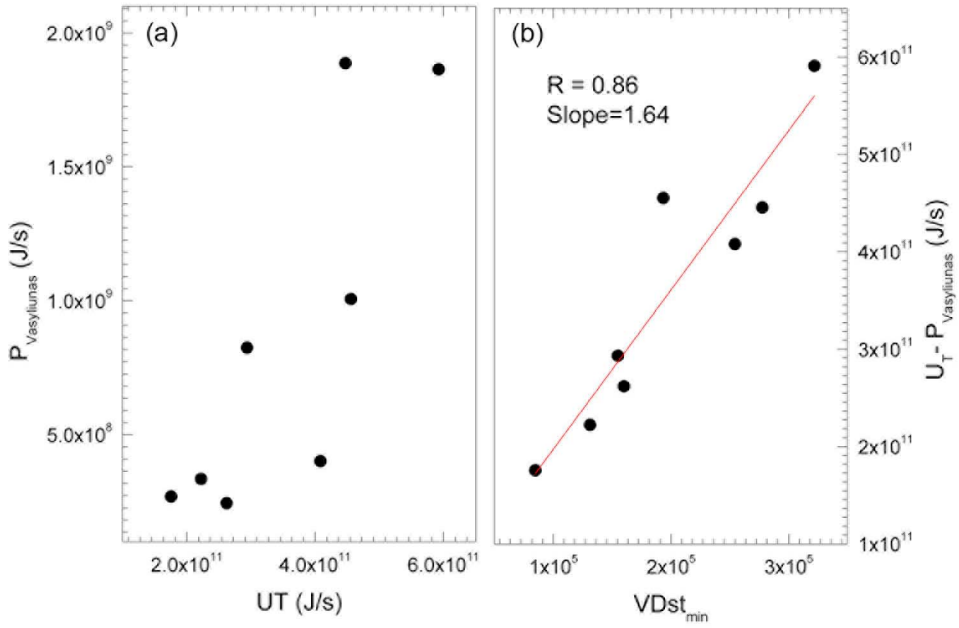

Figure 9. (a) The relationship between U_T and $P_{Vasyliunas}$ for SN cases and (b) the correlation between the stored energy in magnetosphere U_T - $P_{Vasyliunas}$ and V$|Dst|_{\min}$ for NS cases.

Table 2. ER Events During Prolonged Northward Part of SN Clouds

Number	Date[a]	Onset Times (UT)	Maximum AE (nT)	Maximum IMF Magnitude (nT)	Maximum Solar Wind Velocity (km/s)	Maximum Solar Wind Density (n/cc)	Average Clock Angle (deg)	Maximum Epsilon Function (10^{12} J/s)	Minimum Dst (nT)	Delay Time (min)
1	2000/07/16	01:01	1119	48.5	1050	3.4	77.6	12.1	−347	66
2	2000/07/16	03:45	692	40.2	952	11.7	66.6	6.50	−347	170
3	2000/07/16	04:22	929	40.0	949	4.60	55.2	5.00	−347	207
4	2000/08/13	00:05	647	21.0	562	9.50	28.9	1.10	−235	391
5	2000/08/13	03:25	561	20.6	600	27.5	22.0	0.55	−235	591
6	2000/09/18	04:45	430	32.7	871	9.06	39.5	1.37	−203	289
7	2000/11/07	12:40	685	24.2	523	6.40	74.4	1.30	−176	147
8	2001/11/24	22:30	418	19.5	827	8.35	11.6	0.02	−234	420
9	2003/10/31	03:43	1027	26.7	957	X	44.0	X	−432	115
10	2003/10/31	05:30	1683	22.0	1111	X	29.4	X	−432	222
11	2003/10/31	06:19	1827	17.3	1134	X	23.5	X	−432	271
12	2004/11/08	16:35	463	10.6	668	2.28	51.5	0.34	−394	270
13	2004/11/11	17:40	533	11.0	588	14.0	47.3	0.14	−282	182
14	2005/05/15	10:23	608	54.3	979	3.98	51.9	5.93	−305	25

[a]Date format: yyyy/mm/dd.

[42] 3. There were not ERs after 4 h after the onset of the N event.

[43] 4. The associated aurora patches of ERs were usually located in the midnight sector at 60~70° MLAT.

[44] The development of ER disturbances is mainly governed by variations in solar wind conditions and structures [*Lu et al.*, 1998; *Despirak et al.*, 2009]. In the cases shown in the last section, MCs impinged upon the magnetosphere and caused large storms. Many intense ER events occurred during the main phase of storms with southward IMF *Bz*. Typically, the northward turning of the IMF *Bz* terminated/reduced magnetic reconnection and caused the onset of the recovery phase of the major storm. Somewhat weaker ERs occurred during the northward IMF intervals.

[45] The strong correlation between solar wind speed V_{SW} and U_T indicates that the new energy stored in the magnetotail is dependent on V_{SW}. The energy supplied by the solar wind was initially converted to electromagnetic energy (and can be viewed as being stored in the magnetic field, perhaps in the magnetotail) [*Kamide et al.*, 1998]. However, other regions of energy storage have been mentioned by *Tsurutani et al.* [2009]. The intense solar wind controls the driven and unloading of the energy stored in the magnetotail/magnetosphere system.

[46] The maximum |*Dst*| value can be used to roughly evaluate the maximum energy input during the main phase of a storm. The magnetic flux, stored in the tail lobes/magnetosphere during the growth phase, is proportional to the dayside 'merging' electric field [*Shukhtina et al.*, 2005]. Thus the correlation of *Dst* with U_T (see second panel of Figure 2) is interpreted to indicate that the energy input from previous magnetic merging during southward IMF is necessary for the latter occurrence of ERs during northward IMF.

[47] All ERs during prolonged northward IMFs occurred following SN MCs but not following NS MCs. It implies that the level of ERs with northward IMF is controlled by the previous level of magnetic activity, as well as by the structure

Table 3. Lack of ERs During Prolonged Northward Part of SN Clouds

Number	Start Date[a]	Start Times (UT)	End Date[a]	End Times (UT)	Maximum IMF Magnitude (nT)	Maximum Solar Wind Velocity (km/s)	Maximum Solar Wind Density (n/cc)	Minimum Dst (nT)	Maximum AE (nT)
1	1998/02/04	04:30	1998/02/05	22:30	13.8	331	57.8	−36	54
2	1998/03/04	14:18	1998/03/06	06:18	12.9	342	62.9	−28	104
3	1998/06/02	10:36	1998/06/02	15:54	10.6	397	12.5	0	73
4	1998/08/20	10:18	1998/08/21	19:18	15.6	330	14.3	−69	96
5	1999/04/16	20:18	1999/04/17	21:18	21.1	416	22.2	−123	186
6	2001/04/29	01:54	2001/04/29	12:54	11.2	625	8.9	−41	118
7	2001/05/28	11:54	2001/05/29	10:25	10.1	445	6.0	−48	226
8	2001/10/31	21:18	2001/11/02	10:18	11.7	317	17.0	−102	132
9	2002/03/24	03:48	2002/03/25	22:48	20.4	485	27.0	−114	247
10	2002/08/01	11:54	2002/08/01	22:36	14.3	464	22.7	−44	274
11	2005/06/15	05:48	2005/06/16	07:48	10.2	503	11.2	−49	245
12	2005/12/31	14:48	2006/01/01	10:48	10.9	487	7.3	−28	123
13	2007/03/24	03:06	2007/03/24	16:54	8.4	377	23.4	−79	160
14	1996/05/27	15:18	1996/05/29	07:18	16.6	394	58.1	−39	94
15	1996/07/01	17:18	1996/07/02	10:18	12.4	358	26.6	−28	175
16	1997/01/10	05:18	1997/01/11	02:18	23.1	455	71.3	−85	378
17	1997/05/15	09:06	1997/05/16	01:06	19.5	466	13.7	−129	378
18	1997/10/10	23:48	1997/10/12	00:48	11.7	417	9.9	−139	51
19	1997/11/07	15:48	1997/11/08	04:18	18.3	445	10.2	−125	171

[a]Date format: yyyy/mm/dd.

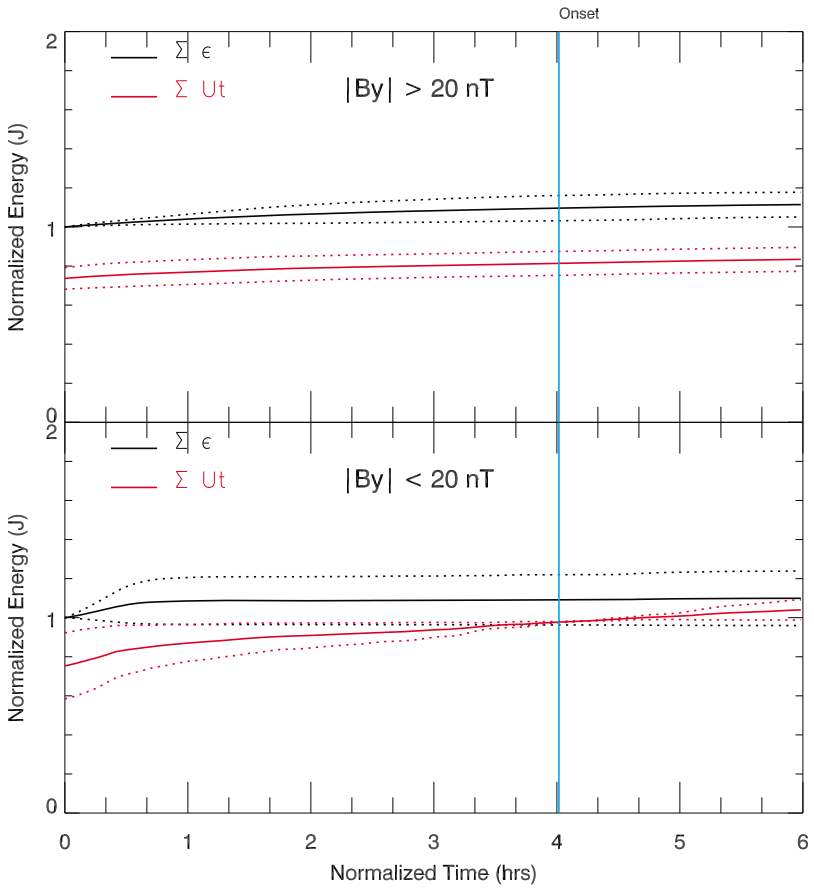

Figure 10. The superpose epoch analysis to investigate the influence of the IMF *By*.

of solar wind. For SN MCs the IMF rotation aids energy input and/or storage. Our results are consistent with the MHD simulation results [*Palmroth et al.*, 2003; *Pulkkinen et al.*, 2007].

[48] The component merging at the low latitude boundary for northward IMF requires a large IMF *By*. *Sandholt et al.* [1998] have suggested that open flux tube production does not switch off entirely until the clock angle falls below 30°~40°, such that during intervals of northward, but *By*-dominated IMF, both open field line (lobe) and closed field line merging may be taking place [*Nishida et al.*, 1998]. *Grocott et al.* [2004], following the work of *Nishida et al.* [1998], suggested that tail merging during northward IMF could be resulted from prolonged dayside merging between terrestrial field lines and a *By*-dominated IMF. *Lee et al.* [2010] consider dayside magnetic reconnection related to finite IMF *By* as a possible mechanism for solar wind energy transfer causing ERs during northward IMF. In contrast, *Echer et al.* [2008] concluded that the primary cause for all major ($Dst < -100$ nT) magnetic storms that occurred during SC23, was IMF B_S fields and not IMF *By* fields. However, we do not see the present results and those above to be in conflict. As found in this study, the cause of the main phase of magnetic storms was indeed IMF *Bz*. However, that does not rule out the possibility that reconnection associated with IMF *By* also occurs, but to a lesser extent. It is also possible that a major magnetic storm caused by IMF *By* exists, but has not been found yet. This could be an interesting study for the interested young researcher.

[49] We use the superpose epoch analysis method to investigate the influence of the IMF *By*. The epoch start time t = 0 is set to be the time of the northward turning of the IMF. We have divided ERs into two groups: $|By| > 20$ nT and $|By| < 20$ nT. The epoch time runs from 4 h before to 2 h after ER onset. The results are shown in Figure 10. In each panel the thick solid line shows the evolution of the median quantity of the parameter, while the thin lines show the upper and lower quantities. We find that the input energy, $\Sigma\varepsilon$, and dissipation energy, ΣU_T, both simultaneously increase for the $|By| > 20$ nT case. The energy input ceases while dissipation continues to increase for $|By| <$ 20 nT. It must be noted, however, that the number of ER events used here are statistically too low to determine if this is the general case or not. An analysis involving more events will be necessary in the future.

[50] In the new coupling function, $Enimf = \alpha N^{-1/12} V_{SW}^{7/3} B^{1/2} + \beta V_{SW} Dst_{\min}$, we mainly take into account the "viscous interaction" term and the magnetotail stored energy term. The first term is based on a solar wind–magnetosphere energy transfer formula for viscous coupling given by *Vasyliunas et al.* [1982]. Its efficiency of solar wind energy input into the Earth's magnetosphere via "viscous interaction" is about $1.0 \times 10^{-2} \sim 1.0 \times 10^{-3}$, which is consistent with the results of *Tsurutani and Gonzalez* [1995]. The second term is obtained from the empirically derived formula that was

obtained by correlating the solar wind parameters, *Dst* and the dissipation energy, U_T. The influence of the IMF *By* is separated from the residual energy in the magnetotail.

5. Conclusions

[51] Magnetospheric ERs occurred during intense northward IMF portions of SN magnetic clouds in the recovery phases of major magnetic storms (the S portion of the magnetic cloud caused the storm main phases). For NS magnetic clouds, there were no ERs detected in the N portions of the clouds (the S portions still created the magnetic storm main phases). Based on these findings, a new coupling function was derived, $Enimf = \alpha N^{-1/12} V_{SW}^{7/3} B^{1/2} + \beta V_{SW} Dst_{min}$. The first term on the right-hand side represents viscous interaction energy input and the second is a magnetotail/magnetosphere energy storage term. A good correlation between the magnetospheric dissipation energy U_T and function $V_{SW}Dst$ demonstrates that the energy associated with ERs under northward IMF conditions is dependent on not only solar wind speed but also the magnitude of energy storage from previous magnetic merging under southward IMF conditions.

6. Final Comments

[52] Our empirical results support a new view of the magnetosphere [see also *Zhou and Tsurutani*, 2001; *Tsurutani and Zhou*, 2003; *Tsurutani et al.*, 2003, 2009]. It is well accepted that southward IMFs and magnetic reconnection [*Dungey*, 1961] is the main mechanism of solar wind energy input into the magnetosphere/magnetotail. Viscous interaction, discussed in this paper, is important, but secondary. Our scenario is that without recent southward IMFs impinging upon the magnetosphere, there will not be ERs. When there are strong N fields (such as the NS cases studied here), any residual stored energy dissipates away slowly without violent ERs occurring. For SN events, energy stored during the S portion of the MC can get released as ERs, but only for up to ~4 h time. The available energy is then spent. What about the vast amount of energy present in the Earth's magnetotail, enough for a dozen ERs/substorms? In our scenario, this energy is not available for usage. Otherwise ERs would occur independent of whether there were S fields prior to the N fields or not. Many articles (too numerous to cite) have indicated that common substorms require IMF *Bs* priming for them to occur. This is essentially the same physical scenario as the shock stimulated ERs discussed here. An interesting question for the space research community is "where is the energy stored, in the magnetotail, the magnetosphere or ionosphere?"

[53] This scenario of short-term energy storage is consistent with past magnetospheric observations. If the IMF is strongly southward, energy is released in the form of ERs and magnetic storms. Are there observations to the contrary? Probably not. If the IMF is moderately southward or $Bz \sim 0$ nT, then shock impingement may cause the sudden occurrence of an ER, during which the stored energy is released. If the IMF has been northward, so very little new energy has been injected and stored, and a shock will not cause the release of an ER. The implications of this scenario are that the rate of energy input is perhaps the most critical parameter for the type of energy release in the magnetosphere/magnetotail.

[54] *Tsurutani et al.* [2009] have posed the same question for the solar case. Does this same scenario work for solar flares? Is it true that the vast energy in the magnetic loops is not used in the energy release (flares) at the Sun, just like the vast energy in the Earth's magnetotail is not used? Then following this line of thought, to predict when a solar flare will occur, it will be necessary to identify the rate of free energy being injected (and stored) into the system. The exact mechanism of energy release (magnetic reconnection) may be secondary in importance.

[55] **Acknowledgments.** We acknowledge the CDAWeb for access to the ACE, Polar, IMAGE, and GOES data. SOPA energetic proton and electron spin-averaged differential flux measurements are afforded by Los Alamos National Laboratory. We especially thank S. B. Mende and Harald Frey for the use of IMAGE FUV WIC data. The AE data are provided by the World Data Center for Geomagnetism at Kyoto University. This work was supported by NSFC grants (41031066), NSFC (41174122) and supported by OPWSRP (201005017). Portions of the work were performed at the Jet Propulsion Laboratory, California Institute of Technology, under contract with NASA.

[56] Philippa Browning thanks the reviewers for their assistance in evaluating this paper.

References

Akasofu, S.-I. (1981), Energy coupling between the solar wind and the magnetosphere, *Space Sci. Rev.*, *28*, 121–190, doi:10.1007/BF00218810.

Axford, W. I., and C. O. Hines (1961), A unifying theory of high-latitude geophysical phenomena and geomagnetic storms, *Can. J. Phys.*, *39*, 1433–1464.

Burch, J. L. (1972), Preconditions for the triggering of polar magnetic substorms by storm sudden commencements, *J. Geophys. Res.*, *77*, 5629–5632, doi:10.1029/JA077i028p05629.

Burlaga, L. F., E. C. Sittler Jr., F. Mariani, and R. Schwenn (1981), Magnetic loop behind an interplanetary shock: Voyager, Helios, and IMP-8 observations, *J. Geophys. Res.*, *86*, 6673–6684, doi:10.1029/JA086iA08p06673.

Chua, D., G. Parks, M. Brittnacher, W. Peria, G. Germany, J. Spann, and C. Carlson (2001), Energy characteristics of auroral electron precipitation: A comparison of substorms and pressure pulse related auroral activity, *J. Geophys. Res.*, *106*, 5945–5956, doi:10.1029/2000JA003027.

Despirak, I. V., A. A. Lubchich, A. G. Yahnin, B. V. Kozelov, and H. K. Biernat (2009), Development of substorm bulges during different solar wind structures, *Ann. Geophys.*, *27*, 1951–1960, doi:10.5194/angeo-27-1951-2009.

Du, A. M., B. T. Tsurutani, and W. Sun (2008), Anomalous geomagnetic storm of 21–22 January 2005: A storm main phase during northward IMFs, *J. Geophys. Res.*, *113*, A10214, doi:10.1029/2008JA013284.

Dungey, J. W. (1961), Interplanetary magnetic field and the auroral zones, *Phys. Rev. Lett.*, *6*, 47–48, doi:10.1103/PhysRevLett.6.47.

Echer, E., W. D. Gonzalez, B. T. Tsurutani, and A. L. C. Gonzalez (2008), Interplanetary conditions causing intense geomagnetic storms (Dst ≤ −100 nT) during solar cycle 23 (1996–2006), *J. Geophys. Res.*, *113*, A05221, doi:10.1029/2007JA012744.

Echer, E., B. T. Tsurutani, F. L. Guarnieri, and J. U. Kozyra (2011), Interplanetary fast forward shocks and their geomagnetic effects: CAWSES events, *J. Atmos. Sol. Terr. Phys.*, *73*, 1330–1338, doi:10.1016/j.jastp.2010.09.020.

Frey, H. U., S. B. Mende, V. Angelopoulos, and E. F. Donovan (2004), Substorm onset observations by IMAGE-FUV, *J. Geophys. Res.*, *109*, A10304, doi:10.1029/2004JA010607.

Gonzalez, W. D., and F. S. Mozer (1974), A quantitative model for the potential resulting from reconnection with an arbitrary interplanetary magnetic field, *J. Geophys. Res.*, *79*, 4186–4194, doi:10.1029/JA079i028p04186.

Gonzalez, W. D., and B. T. Tsurutani (1987), Criteria of interplanetary causing intense magnetic storms (Dst < −100nT), *Planet. Space Sci.*, *35*, 1101–1109, doi:10.1016/0032-0633(87)90015-8.

Gonzalez, W. D., B. T. Tsurutani, A. L. C. Gonzalez, E. J. Smith, F. Tang, and S.-I. Akasofu (1989), Solar wind–magnetosphere coupling during intense magnetic storms (1978–1979), *J. Geophys. Res.*, *94*, 8835–8851, doi:10.1029/JA094iA07p08835.

Gonzalez, W. D., J. A. Joselyn, Y. Kamide, H. W. Kroehl, G. Rostoker, B. T. Tsurutani, and V. M. Vasyliunas (1994), What is a geomagnetic storm?, *J. Geophys. Res.*, *99*, 5771–5792, doi:10.1029/93JA02867.

Grocott, A., S. V. Badman, S. W. H. Cowley, T. K. Yeoman, and P. J. Cripps (2004), The influence of IMF By on the nature of the nightside high-latitude ionospheric flow during intervals of positive IMF Bz, *Ann. Geophys.*, *22*, 1755–1764, doi:10.5194/angeo-22-1755-2004.

Henderson, M. G., G. D. Reeves, R. D. Belian, and J. S. Murphy (1996), Observations of magnetospheric substorms with no apparent solar wind/IMF trigger, *J. Geophys. Res.*, *101*, 10,773–10,791, doi:10.1029/96JA00186.

Heppner, J. P. (1955), Note on the occurrence of world-wide SSCs during the onset of negative bays at College, Alaska, *J. Geophys. Res.*, *60*, 29–32, doi:10.1029/JZ060i001p00029.

Kamide, Y., et al. (1998), Current understanding of magnetic storms: Storm-substorm relationships, *J. Geophys. Res.*, *103*, 17,705–17,728, doi:10.1029/98JA01426.

Kawasaki, K., S.-I. Akasofu, F. Yasuhara, and C.-I. Meng (1971), Storm sudden commencements and polar magnetic substorms, *J. Geophys. Res.*, *76*, 6781–6789, doi:10.1029/JA076i028p06781.

Lee, D.-Y., K.-C. Choi, S. Ohtani, J. H. Lee, K. C. Kim, K. S. Park, and K.-H. Kim (2010), Can intense substorms occur under northward IMF conditions?, *J. Geophys. Res.*, *115*, A01211, doi:10.1029/2009JA014480.

Lepping, R. P., D. B. Berdichevsky, C.-C. Wu, A. Szabo, T. Narock, F. Mariani, A. J. Lazarus, and A. J. Quivers (2006), A summary of Wind magnetic clouds for years 1995–2003: Model-fitted parameters, associated errors and classifications, *Ann. Geophys.*, *24*, 215–245, doi:10.5194/angeo-24-215-2006.

Lu, G., et al. (1998), Global energy deposition during the January 1997 magnetic cloud event, *J. Geophys. Res.*, *103*, 11,685–11,694, doi:10.1029/98JA00897.

Lyons, L. R. (2000), Geomagnetic disturbances: Characteristics of, distinction between types, and relations to interplanetary conditions, *J. Atmos. Sol. Terr. Phys.*, *62*, 1087–1114, doi:10.1016/S1364-6826(00)00097-3.

Mannucci, A. J., B. T. Tsurutani, M. A. Abdu, W. D. Gonzalez, A. Komjathy, E. Echer, B. A. Iijima, G. Crowley, and D. Anderson (2008), Superposed epoch analysis of the dayside ionospheric response to four intense geomagnetic storms, *J. Geophys. Res.*, *113*, A00A02, doi:10.1029/2007JA012732.

Meurant, M., J.-C. Gérard, C. Blockx, V. Coumans, B. Hubert, M. Connors, L. R. Lyons, and E. Donovan (2005), Comparison of intense nightside shock-induced precipitation and substorm activity, *J. Geophys. Res.*, *110*, A07228, doi:10.1029/2004JA010916.

Newell, P. T., T. Sotirelis, K. Liou, C.-I. Meng, and F. J. Rich (2007), A nearly universal solar wind–magnetosphere coupling function inferred from 10 magnetospheric state variables, *J. Geophys. Res.*, *112*, A01206, doi:10.1029/2006JA012015.

Newell, P. T., T. Sotirelis, K. Liou, and F. J. Rich (2008), Pairs of solar wind–magnetosphere coupling functions: Combining a merging term with a viscous term works best, *J. Geophys. Res.*, *113*, A04218, doi:10.1029/2007JA012825.

Nieves-Chinchilla, T., M. A. Hidalgo, and J. Sequeiros (2005), Magnetic clouds observed at 1 AU during the period 2000–2003, *Sol. Phys.*, *232*, 105–126, doi:10.1007/s11207-005-1593-5.

Nishida, A., T. Mukai, T. Yamamoto, S. Kokubun, and K. Maezawa (1998), A unified model of the magnetotail convection in geomagnetically quiet and active times, *J. Geophys. Res.*, *103*, 4409–4418, doi:10.1029/97JA01617.

Palmroth, M., T. I. Pulkkinen, P. Janhunen, and C.-C. Wu (2003), Stormtime energy transfer in global MHD simulation, *J. Geophys. Res.*, *108*(A1), 1048, doi:10.1029/2002JA009446.

Perreault, P., and S.-I. Akasofu (1978), A study of geomagnetic storms, *Geophys. J. R. Astron. Soc.*, *54*, 547–573.

Pulkkinen, T. I., M. Palmroth, and R. L. McPherron (2007), What drives magnetospheric activity under northward IMF conditions?, *Geophys. Res. Lett.*, *34*, L18104, doi:10.1029/2007GL030619.

Sandholt, P. E., C. J. Farrugia, J. Moen, Ø. Noraberg, B. Lybekk, T. Sten, and T. Hansen (1998), A classification of dayside auroral forms and activities as a function of IMF orientation, *J. Geophys. Res.*, *103*, 23,325–23,345.

Schieldge, J. P., and G. L. Siscoe (1970), A correlation of the occurrence of simultaneous sudden magnetospheric compressions and geomagnetic bay onsets with selected geophysical indices, *J. Atmos. Terr. Phys.*, *32*, 1819–1830, doi:10.1016/0021-9169(70)90139-X.

Shue, J.-H., J. K. Chao, H. C. Fu, C. T. Russell, P. Song, K. K. Khurana, and H. J. Singer (1997), A new functional form to study the solar wind control of the magnetopause size and shape, *J. Geophys. Res.*, *102*, 9497–9511.

Shukhtina, M. A., N. P. Dmitrieva, N. G. Popova, V. A. Sergeev, A. G. Yahnin, and I. V. Despirak (2005), Observational evidence of the loading-unloading substorm scheme, *Geophys. Res. Lett.*, *32*, L17107, doi:10.1029/2005GL023779.

Stone, E. C., et al. (1998), The Advanced Composition Explorer, *Space Sci. Rev.*, *86*, 1–22, doi:10.1023/A:1005082526237.

Tsurutani, B. T., and W. D. Gonzalez (1994), The causes of geomagnetic storms during solar maxima, *Eos Trans. AGU*, *75*(5), 49, doi:10.1029/94EO00468.

Tsurutani, B. T., and W. D. Gonzalez (1995), The efficiency of viscous interaction between the solar wind and the magnetosphere during intense northward IMF events, *Geophys. Res. Lett.*, *22*, 663–666, doi:10.1029/95GL00205.

Tsurutani, B. T., and W. D. Gonzalez (1997), The interplanetary causes of magnetic storms: A review, in *Magnetic Storms*, *Geophys. Monogr. Ser.*, vol. 98, edited by B. T. Tsurutani et al., pp. 77–90, AGU, Washington, D. C.

Tsurutani, B. T., and X.-Y. Zhou (2003), Interplanetary shock triggering of substorms: Wind and Polar, *Adv. Space Res.*, *31*, 1063–1067, doi:10.1016/S0273-1177(02)00796-2.

Tsurutani, B. T., W. D. Gonzalez, F. Tang, S.-I. Akasofu, and E. J. Smith (1988), Origin of interplanetary southward magnetic fields responsible for major magnetic storms near solar maximum (l978–l979), *J. Geophys. Res.*, *93*, 8519–8531, doi:10.1029/JA093iA08p08519.

Tsurutani, B. T., G. S. Lakhina, D. Winterhalter, J. K. Arballo, C. Galvan, and R. Sakurai (1999), Energetic particle cross-field diffusion: Interaction with magnetic decreases (MDs), *Nonlinear Processes Geophys.*, *6*, 235–242, doi:10.5194/npg-6-235-1999.

Tsurutani, B. T., X.-Y. Zhou, V. M. Vasyliunas, G. Haerendel, J. K. Arballo, and G. S. Lakhina (2001), Interplanetary shocks, magnetopause boundary layers and dayside auroras: The importance of a very small magnetospheric region, *Surv. Geophys.*, *22*, 101–130, doi:10.1023/A:1012952414384.

Tsurutani, B. T., X.-Y. Zhou, and W. D. Gonzalez (2003), A lack of substorm expansion phases during magnetic storms induced by magnetic cloud, in *The Storm-Substorm Relationship*, *Geophys. Monogr. Ser.*, vol. 142, edited by Y. Kamide et al., pp. 23–36, AGU, Washington, D. C., doi:10.1029/142GM03.

Tsurutani, B. T., K. Shibata, S.-I. Akasofu, and M. Oka (2009), A two-step scenario for both solar flares and magnetospheric substorms: Short duration energy storage, *Earth Planets Space*, *61*, 555–559.

Vasyliunas, V. M., J. R. Kan, G. L. Siscoe, and S.-I. Akasofu (1982), Scaling relations governing magnetospheric energy transfer, *Planet. Space Sci.*, *30*, 359–365, doi:10.1016/0032-0633(82)90041-1.

Wang, Y., G. Zhou, P. Ye, S. Wang, and J. Wang (2006), A study of the orientation of interplanetary magnetic clouds and solar filaments, *Astrophys. J.*, *651*, 1245–1255, doi:10.1086/507668.

Xue, X. H., Y. Wang, P. Z. Ye, S. Wang, and M. Xiong (2005), Analysis on the interplanetary causes of the great magnetic storms in solar maximum (2000–2001), *Planet. Space Sci.*, *53*, 443–457, doi:10.1016/j.pss.2004.10.002.

Zhou, X., and B. T. Tsurutani (2001), Interplanetary shock triggering of nightside geomagnetic activity: Substorms, pseudobreakups, and quiescent events, *J. Geophys. Res.*, *106*, 18,957–18,967, doi:10.1029/2000JA003028.

A. M. Du, Institute of Geology and Geophysics, Chinese Academy of Sciences, Beijing 100029, China. (amdu@mail.iggcas.ac.cn)

W. Sun, Geophysical Institute, University of Alaska Fairbanks, Fairbanks, AK 99775, USA.

B. T. Tsurutani, Jet Propulsion Laboratory, California Institute of Technology, Pasadena, CA 91109, USA.